We are IntechOpen, the world's leading publisher of Open Access books Built by scientists, for scientists

4,800
Open access books available

122,000
International authors and editors

135M
Downloads

Our authors are among the

154
Countries delivered to

TOP 1%
most cited scientists

12.2%
Contributors from top 500 universities

CLARIVATE ANALYTICS BOOK CITATION INDEX INDEXED

WEB OF SCIENCE™

Selection of our books indexed in the Book Citation Index in Web of Science™ Core Collection (BKCI)

Interested in publishing with us?
Contact book.department@intechopen.com

Numbers displayed above are based on latest data collected.
For more information visit www.intechopen.com

15

RF-MEMS based Tuner for microwave and millimeterwave applications

David Dubuc[1,2] and Katia Grenier[1]
[1]*LAAS-CNRS, Toulouse and* [2]*University of Toulouse*
France

1. Introduction

This chapter sets out the basics and applications of impedance tuner for microwave and millimeterwave applications. Engineering examples, based on innovative and up-to-date Radio-Frequency MicroElectroMechanical Systems (RF-MEMS) technologies, are used to illustrate theoretical and practical principles. An explicit, comprehensive and efficient design methodology of impedance tuners is furthermore detailed. This generic design procedure is illustrated by the design of a tuner building block and followed by the description of appropriate measurements. Finally the capabilities of RF-MEMS based Impedance tuner issued from the state of the art are briefly reviewed and are followed by global conclusions.
The purposes of this chapter are then to give to the readers comprehensive informations on:

- The basics and applications of microwave and millimeterwave impedance tuners,
- The architectures of tuners,
- The implementation of tuner thanks to RF-MEMS technology,
- The design and characterization methodologies.

2. Basic definitions of Impedance Tuner

2.1 Applications and Basic definitions

Impedance matching is one of the key activities of microwave designers. Targeting maximum power transmission and/or low noise operation, impedance matching networks widely take place in all RF, microwave and millimeterwave systems. The corresponding design techniques are now well established and described in plenty of microwave books (Pozar, 2005; Collin, 2001).
For a decade, with the increase of microwave applications, requirements in term of system-reconfigurability have raised the level of complexity of circuits and especially of matching circuits. In addition to existing design constraints (detailed below), the ability of tunability without any loose of performances, and even with improved performances, has become mandatory. This is accomplished in conjunction with the use of new technologies to fulfill integration and increased frequency operation trends (Dubuc et al., 2004).

This actual trend gives rise to the development of new kinds of integrated microwave passive networks, which match/generate impedances with reconfigurable ability. Two major applications, presented in the Figure 1 and detailed below, take full benefit from these high performances and integrated circuits: (1) tunable matching networks in reconfigurable and smart RF-microsystem, and (2) impedances generators, which exhibit wide range of impedance values for devices characterization.

The Figure 1 (a) presents a reconfigurable front-end system, where impedance tuning circuits (referred in this chapter as *impedance tuner* or simply *tuner*) correspond to the key blocks in order to assure tunability under high efficiency operation (mainly high received-transmit power and low noise operation) (Rebeiz, 2003). For this application, the main features of such circuits may be listed as:

- the set of source and load impedances, which can be matched. This can be presented as the number of covered quadrants of the Smith Chart or simply by the impedance tuning range (both for the real and imaginary parts),
- the frequency bandwidth, as reconfigurability of operating frequency is concerned here,
- the insertion losses or the power efficiency of the tuner,
- the power handling capabilities,
- the DC –power consumption, as tunable-switchable elements are mandatory for tunability,
- the integration level.

As far as this last characteristic is concerned, an entire integrated system vision is considered in this chapter. This means that impedance tuners may be co-integrated with Integrated Circuits (IC). Tremendous consequences on potential applications may occur, such as the use of integrated impedance tuner for smart telecommunication systems or for millimeterwave instrumentation.

The massive integration of tuners within microsystems results in adaptative RF front-end, where functionalities can be reconfigured as well as operating frequencies (Qiao et al., 2005). The tuning capabilities of matching network gives rise to higher system efficiency and wider bandwidth. Moreover, on-wafer tuning can be also employed to compensate variations due to aging, temperature drift and unit-to-unit dispersion.

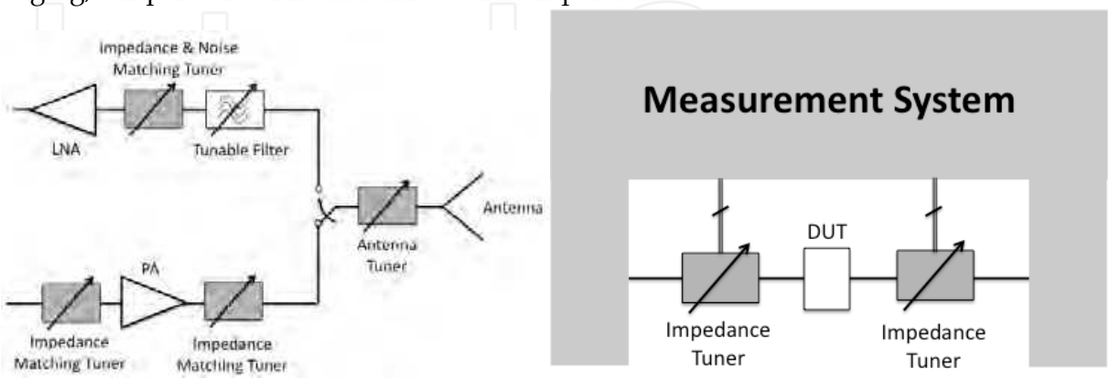

(a) (b)

Fig. 1. Typical applications of Impedance Tuners : (a) reconfigurable front end system (b) integrated instrumentation systems

For instrumentation application, the integration of tuner circuits as close as possible to the device under test (DUT) also enlarges the measurements capabilities. The parasitic reduction in the test chain results in a rise of the maximum frequency operation: RF-MEMS tuners up to W-band have been successfully demonstrated (Vähä-Heikkilä et al., 2005). Moreover, the reduction of losses between the tuner and the DUT translates into an improvement of achievable VSWR often mandatory to provide an accurate modeling (Tagro et al., 2008). The Figure 1. (b) presents such systems : the tuners generate impedance loci featuring high impedance coverage under high frequency operation. Applications for noise or load-pull measurements can be envisioned.

2.2 Architecture of Impedance tuner

Impedance tuner architectures derive from fixed matching circuits. In this chapter, we focus on circuits able to operate in the microwave and millimeterwave domain, typically at frequencies above the X-band. Transmission lines-based circuits, which are more suitable at frequency higher than 6 GHz, are consequently discussed. Nevertheless, the next paragraph will be dedicated to semi-lumped tuner as tunability concept and expected performances can simply be introduced.

As far as lumped-elements solutions are concerned, such tuners are generally limited to 6GHz, but their associated concepts are very illustrative as they can be simply extended to all kinds of tuner. The figure 2 presents a generic reconfigurable impedance matching circuit (Pozar, 2005), which can be used as a tuner thanks to reconfigurable capacitors or inductors. Various solutions for elements' tuning are also illustrated both for inductors and capacitors. Banks of digitally commuted elements correspond to an efficient way of tuning (Papapolymerou et al., 2003).

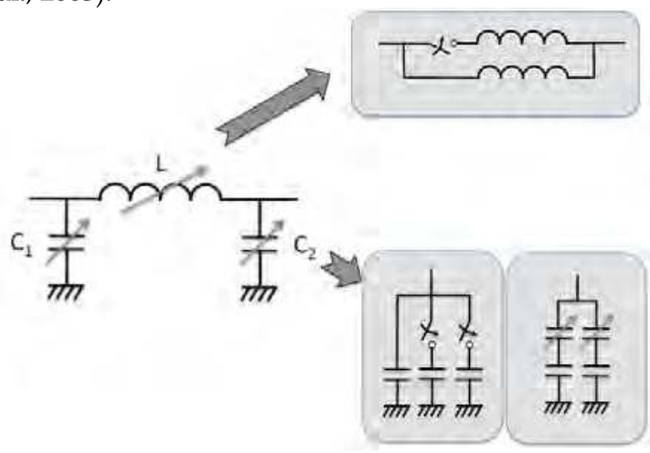

Fig. 2. Typical Lumped-Impedance Tuners

Tuning of only one element of the circuit described in figure 2 can result into a wide impedance/operating frequency tuning. The reconfigurable ability of a 4:1 impedance matching circuit has been investigated (Rebeiz, 2003). Variation of only 30 to 50% of C_2 (L and C_1 are fixed) translates into 60 to 100% of the impedance variation (for a fixed frequency) or more than 100% of fractional bandwidth (compared with 10% bandwidth for fixed elements), for a fixed set of source and load impedances.

For X-band and above (up to W-band), tuner architectures mainly involve Transmission-Lines (TL) and varactors. This type of impedance tuner is based on well-known single-double-triple-stubs impedance matching's architectures (Collin, 2001). The tuning were firstly realized using mechanical devices with either coaxial or waveguides structures, which results in cumbersome solutions requiring motors for automatic control. To integrate reconfigurable tuner, the tuning was then achieved thanks to switching elements and/or variable capacitors (diode and/or transistors), which commute or reconfigure the electrical length and/or the characteristic impedance of TL/stubs.
The figure 3. (a) presents a basic example of 3 switchable stubs featuring different electrical characteristics. To minimize the occupied space, electrical length of stubs can also be tuned with serial switches (figure 3. (b)) or shunt ones (figure 3. (c)).
Reconfigurable stub can also be realized by using switchable loading capacitor at the end of the stub or distributed along (figure 3.(d)). In specific conditions, described in the paragraph 4 of this chapter, the periodic capacitive loading translates into a equivalent TL with tunable electrical length (and characteristic impedance). The figure 4 presents such a tunable distributed transmission line, which represents the key element for multiple stubs matching network.

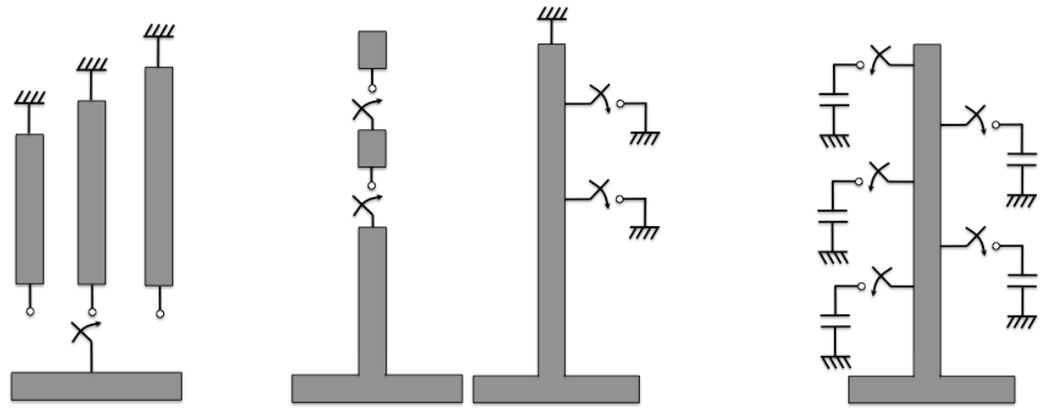

Fig. 3. Tunable stubs, which serve as building blocs of impedance tuners.

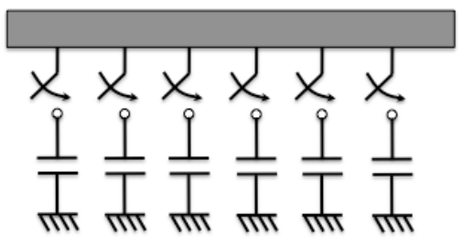
Fig. 4. Tunable Distributed Transmission Line

PIN diodes, Field Effect Transistors or switchable capacitors (also named varactor : variable capacitor) can also be exploited to tune the impedance and/or electrical length of TL. The figure 5 (a) presents a periodically loaded TL, where reactive loading elements modify the TL-phase velocity and its characteristic impedance. This topology can serve as a matching network and consequently as a tuner with limited impedance coverage. It is however suitable for power applications. The RF-current carried through switched distributed

capacitors is indeed weaker than with any other architecture (such as described in figure 3), which results in improved power handling capabilities.
More advanced impedance coverage can be achieved thanks to the use of stubs: the more the numbers of stubs take place, the wider the impedance coverage and bandwidth become (Collin, 2001). The counterpart is nevertheless an increased occupied surface and then a rise of insertion losses. This is illustrated by the schematic of figure 5. (b), which presents a reconfigurable single stub using the same principle of operation of the TL described in figure 5. (a).

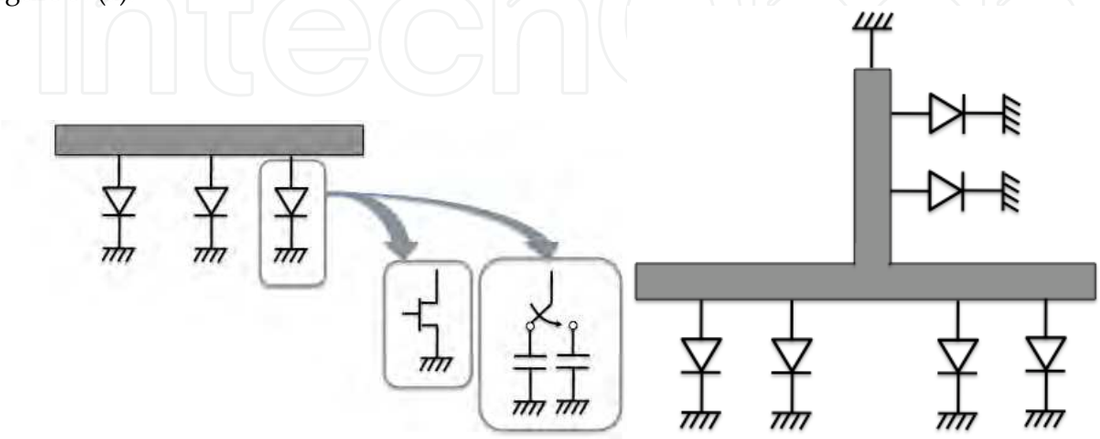

(a) (b)

Fig. 5. PIN diode, Field Effect Transistors and varactor–based impedance tuners.

The bandwidth of a tuner is also an important feature, which impacts on its architecture. The bandwidth of a lumped matching network depends on the ratio of the impedances to match. Large difference in the values of source and load impedances translates indeed into a high resonant behavior and then low circuit's bandwidth. This result can simply be pointed out with lumped circuits but is also true for distributed network.
One solution to enhance the bandwidth corresponds to use multistage transformers, for which the impedance ratio of each stage is divided by the number of stages. For TL-based-architecture, this multistage technique is built on "N-section Chebyshev impedance transformers" method for example (Collin, 2001; Pozar, 2005). As an illustration, thanks to lumped matching network as described in figure 2, the matching of impedances with a ratio of 4:1 results in a 10% fractional bandwidth for 1-stage and 30% thanks to 3-stages topology (Rebeiz, 2003). Of course, the tuning of elements can be applied in this case, not to tune the impedances to match but to improve the bandwidth (100% or more of the fractional bandwidth can be reached thanks to the tuning of the matching network). The price to pay is nevertheless an increase of the occupied surface and consequently the losses. This point limits the number of matching section to 2 or 3 stages depending on the requirements and chosen technology.
Another gain, that can be expected from multistage-tuner, corresponds to power capabilities. Increasing the bandwidth by a reduction of the resonant behavior of circuits indeed translates into a reduction of both current and voltage in the network. For fixed I-V constraints on devices and especially on RF-MEMS varactors, for which reliability highly depends on currents passing through and voltages across, the power can be raised. This explains why distributed TL, loaded with RF-MEMS varactors, corresponds to a good

candidate for high bandwidth tuner (Shen & Barker, 2005) and/or medium power applications (Lu et al., 2005).
The next paragraph presents the RF-MEMS technology, which is particularly attracting for tuner integration because of the available reconfigurable devices and the high performances they exhibit (Rebeiz, 2003).

3. RF-MEMS Technology

The selection of a technology for tuner applications is motivated by the envisioned performances expected for the circuits inside the whole system. As integration is required to address attractive applications of reconfigurable frond-end and advanced instrumentation systems, cumbersome rectangular waveguide solution with mechanical screw or ferrite for tunability is excluded. As far as high RF-performances is expected (the benefit from the integration of tuner should not be suppressed by a loose of performances), the tunability must reside in high quality components in term of:

- low losses, to reach high VSWR, high impedance coverage, low added noise and high power efficiency,
- high integration level, to assure a co-integration with active circuits and permit the integration of periodic loaded structures,
- low power consumption, as integration of tens of switches/varactors is required per matching network and tens of them per microsystems,
- high linearity to address load-pull applications as well as power amplifier matching ones.

The figure 6 presents these 4 performances for 3 different technologies which are suitable for tunability implementation: using PIN diodes or Field Effect Transistors (MMIC), using rectangular waveguide solutions which are generally based on the use of ferrite and finally the RF-MEMS technology, which corresponds to an excellent challenger for tuner application.

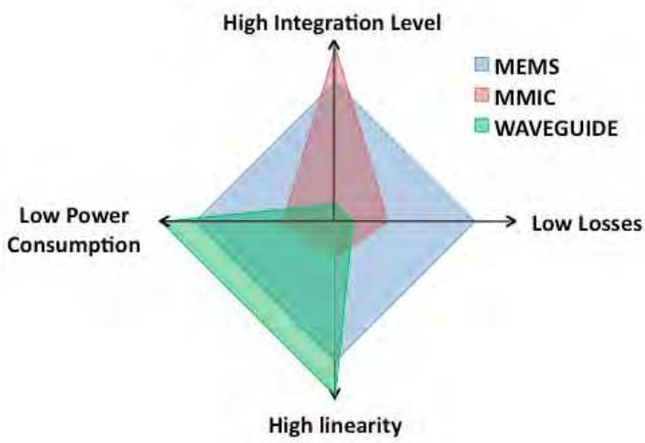

Fig. 6. Achievable tuners' performances vs technologies

One of the key features of RF-MEMS resides in their high quality factors of the resulting varactors. As already discussed, the tuner's topologies generally involve varactors and transmission lines and their losses greatly impact the overall insertion losses, more

especially as the resonant behavior of circuits is intentionally high. The figure 7 illustrates the impact of capacitor quality factor and line lineic losses on the insertion losses at 20GHz for a capacitively loaded stub (see the insert of the figure 7). It is then shown that quality factor of 30 or higher is mandatory for typical transmission line losses. This, once again, highlights the RF-MEMS devices, which generally exhibit quality factors greatly higher than 30, whereas it corresponds to the maximum value obtained thanks to MMIC varactors built with FET transistors.

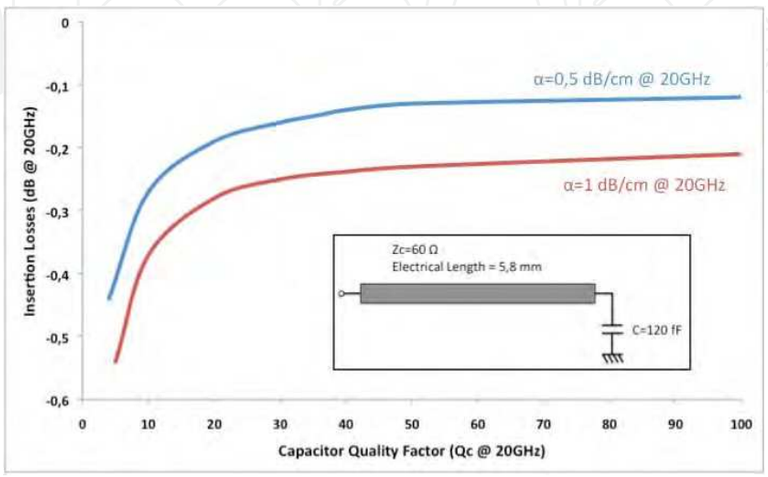

Fig. 7. Impact of capacitor's quality factor on the capacitively loaded stub insertion losses.

Numerous RF-MEMS-technologies have been developed all around the world to fulfill specific requirements (frequency operation, power handling, RF-performances, ...) (Rebeiz, 2003). The next two paragraphs present one of them, which has been developed at the LAAS-CNRS toward the integration of reconfigurable microwave passive networks over silicon active ICs (Grenier et al., 2005).

3.1 RF MEMS devices technology

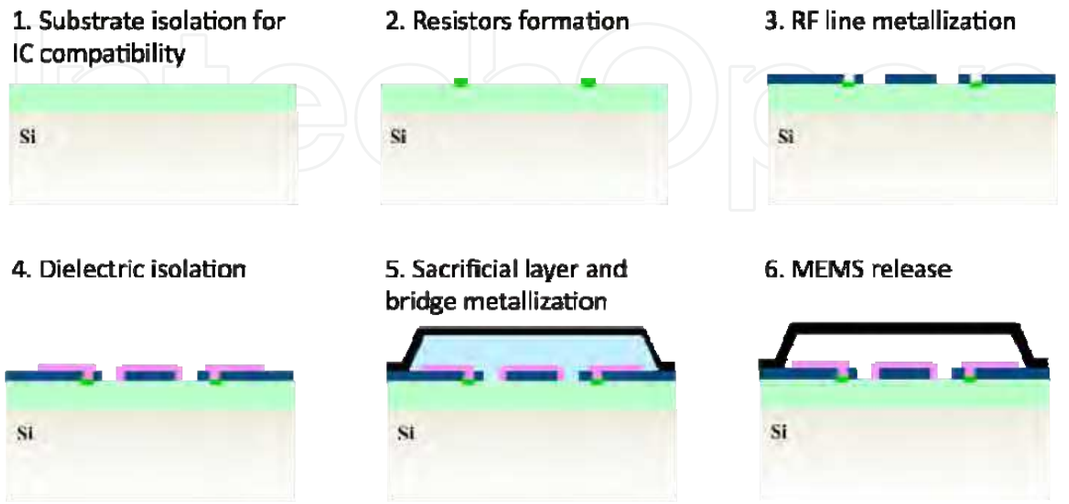

Fig. 8. Process flow of RF MEMS devices

The RF-MEMS technology described in this chapter was specifically developed in order to fulfill the previously mentioned requirements in terms of IC compatibility, low losses, high isolation as well as medium power ability. The corresponding process flow is divided in six major steps, as illustrated in Fig. 8. It includes isolation from the lossy substrate, metallization for the RF lines and the mobile membrane, as well as a thin dielectric layer and integrated resistors.

First, a polymer layer of 15 µm thick is spin-coated on top of a silicon wafer. It provides an excellent isolation between the future MEMS devices and the substrate (Grenier et al., 2004), which may include ICs for complete reconfigurable systems integration (Busquere et al., 2006). This elevation from the substrate partly confines indeed the electrical fields into a lower loss tangent material instead of the lossy silicon. The polymer "Benzocyclobuten" from Dow Chemicals, which exhibits a loss tangent close to 2.10^{-4} in the GHz range, is used. After its spin-coating, a polymerization procedure is realized at 250°C under nitrogen flow, during one hour.

An evaporated germanium layer is then patterned to realize integrated resistors. Other kinds of integrated resistors can be used such as silicon-chrome (Vähä-Heikkilä & Rebeiz, 2004-a). Nevertheless, Germanium material exhibits high value of resistivity (Grenier et al., 2007), which is in favor for low losses operation. Next step consists in the deposition of the RF lines metallization. In order to lower the metallic losses and also allow power handling through the MEMS devices, a high thickness of gold, 2 µm at least, is elaborated. Instead of an electroplating technique, which is particularly suitable for high metal thickness formation but suffers from roughness, a lift-off procedure is employed. The consequent minimization of the roughness enhances the contact quality between the metallic membrane and the MEMS dielectric and thus improves the accessible capacitive ratio.

In a fourth step, the MEMS dielectric of 0.25 µm thick is performed at 300°C by Plasma Enhanced Chemical Vapor Deposition (PECVD). After its delimitation by dry etching, a sacrificial layer is deposited and patterned. A specific care is given to this layer in order:

- to sustain the next technological steps,
- to obtain a flat MEMS bridge; several depositions and photolithographic steps are consequently required to take the RF lines relief into account,
- and to assure a good strength of the membrane anchorages.

As an air gap of 3 µm between the MEMS bridge and the central conductor of the RF line is targeted, the sacrificial layer is defined with such a thickness.

The metallic membrane is then obtained with two successive depositions: an evaporated gold layer of 0.2 µm, followed by an electroplated one of 1.8 µm. The evaporated metal, which exhibits important internal stress, is minimized to drastically decrease any risk of membrane's buckling. The gold bridge is then obtained with a classical wet etching.

The next and most critical step of the process consists in the release of the MEMS structure. It corresponds to the suppression of the sacrificial layer through chemical etching, followed by its drying.

Fig. 9 indicates the photography of a realized RF MEMS switch (which corresponds in fact to a varactor with a high capacitor ratio). This example includes a metallic membrane placed on top of a coplanar waveguide, with four membrane's anchorages and four integrated resistors. The bridge is composed of a central part, which assures the capacitor values, and two actuation electrodes located apart the line, which large surface decreases the required actuation voltage (close to 20-25 V generally) (Ducarouge et al., 2004).

Such a MEMS switch may be modeled with an RLC electrical schematic, which is embedded between two transmission lines, as illustrated in the drawing of

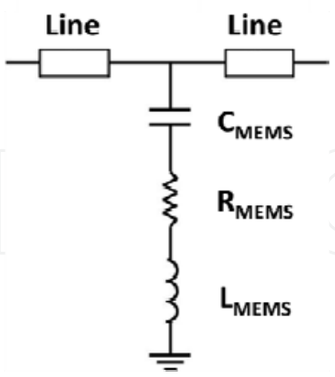

Components		Values
Lines:	Z0	48Ω
	$\varepsilon_{r,eff}$	3.085
	Length	100µm
L_{MEMS}		28 pH
C_{MEMS}	up	70 fF
	down	2330 fF
	ratio	33
Q @ 20GHz	up	>100
	down	28
R_{MEMS}		0.12 Ω

Table 1. Electrical model of the RF MEMS switch

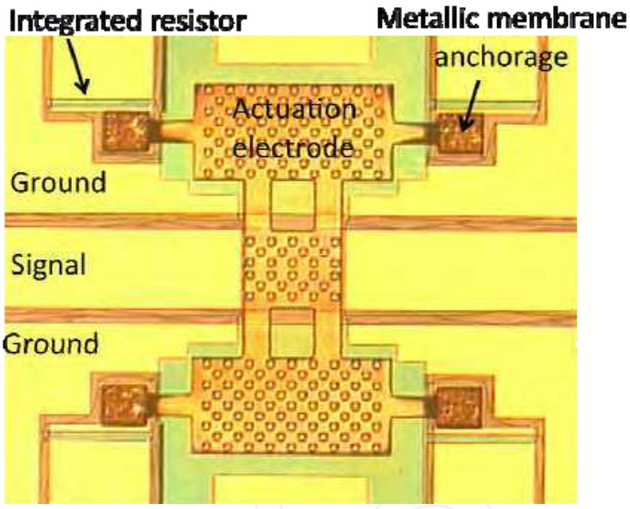

Fig. 9. Photography of a classical RF MEMS switch

The R_{MEMS} resistor corresponds to losses in the metallic membrane. The L_{MEMS} inductor is due (1) to the connecting arms between the central part of the bridge and the actuation electrodes and (2) to the suspension arms of the membrane itself. The capacitor's value C_{MEMS} depends of the state of the bridge and of the regarding surface. Its ratio in the "up" and "down" states is a good indicator about the contact quality of the MEMS switch and the corresponding technology.

As far as the access lines are concerned, they present a characteristic impedance close to 50 Ohm with an effective relative permittivity of 3 and a length of 100 µm.

The achievable RF performances of such an RF MEMS switch are presented in **Fig. 10** in both up and down states of the membrane. At 20 GHz, the insertion losses are close to 0.25dB (which include the contribution of the 200 µm long lines placed apart the membrane), whereas the isolation reaches 50 dB. The RF MEMS switch exhibits

consequently very low losses and high isolation, with a capacitor ratio of 33. Power tests have demonstrated that such an RF MEMS may handle up to 1W during 30 millions of cycles in hot switching.

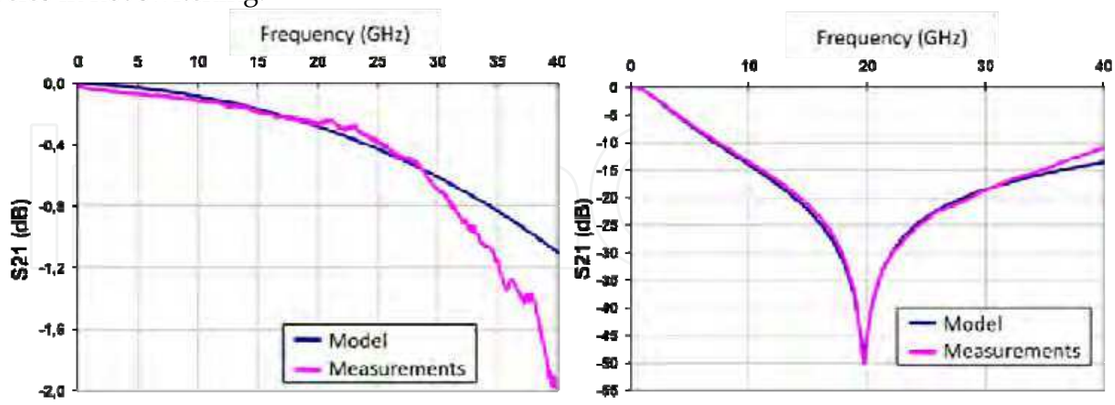

(a) (b)

Fig. 10. Simulations and measurements of an elementary RF MEMS switch in (a) up and (b) down positions

A good agreement between modeling and measurements is achieved for both insertion losses (Fig. 10.a) and isolation (Fig. 10.b). These results validate the simple model used for the RF MEMS switch. A better fit at high frequency could however be reached if additional parasitic elements were considered, but it would highly complex the electrical model.

Depending on the technology, device architecture and targeted application, various reliability performances under low (in the milliWatt range) and medium (in the Watt range) power in hot or cold switching (the RF-power is on or off – respectively- during the MEMS switching) can be found in the literature. The reliability of RF-MEMS is actually one major concern (together with packaging issues) of the RF-MEMS researches. Considered solutions aims to optimize as much as possible the different parameters, which limits the lifetime of RF-MEMS devices/circuits such as:

(1) the actuation scheme of the devices. The frequency and the duty cycle of the biasing voltage have a high impact on the MEMS reliability (Van Spengen et al., 2002; Melle et al., 2005),
(2) the dielectric configuration, which is subject to charging. Some solutions to decrease the charging and/or enhance the discharging have already been proposed, such as adding holes (Goldsmith et al., 2007) or carbon-nanotubes (Bordas et al., 2007-b) in the dielectric for examples. In any case, dielectric charging is one major concern for high reliable RF-MEMS circuits,
(3) the thermal effects in metal lines under medium RF-power. The consequent heat induces deformation of the mobile membrane (and even buckling), which results in mechanical failure (Bordas et al., 2007-a),
(4) the electro-migration, as high current density, which is induced in metal line under medium RF-power, results in alteration of metallization and then alters the operation of the device.

As far as the elaboration of tuner is concerned, many identical MEMS structures are required to form the complete circuit. However, some technological dispersions during the fabrication of MEMS structures may not be totally avoided, especially the contact quality

between the metallic membrane and the MEM dielectric. Moreover as defined previously in (Shen & Barker, 2005), capacitive ratio of 2-5:1 are required. Consequently, new MEMS varactors, which integrate Metal-Insulator-Metal (MIM) capacitors, have been developed.

3.2 RF MEMS varactor and associated technology

Based on the previous RF-MEMS devices, MIM capacitors have been added. They are placed between the ground planes and the membrane anchorages, as indicated in **Fig. 11**. They present the high advantage of being very compact, contrary to Metal-Air-Metal (MAM) capacitors (Vähä-Heikkilä & Rebeiz, 2004-a), but at the detriment of quality factor due to additional dielectric losses.

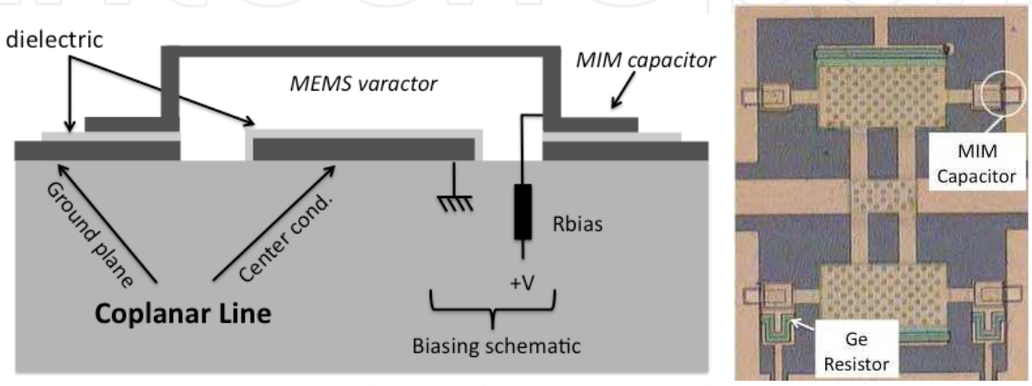

Fig. 11. Cross section view and photography of a RF MEMS switch with integrated MIM capacitors

The precedent technological process flow has consequently been modified to integrate these MIM capacitors. Two additional steps are required. After the elaboration of the RF lines, the MIM dielectric (Silicon Nitride) is deposited by PECVD and patterned. A top metallization is realized by evaporation and delimited. The MEMS process restarts then with the deposition of the MEM dielectric and continue until the final release of the structure. Because of technological limitations, MIM capacitors have to present a value equal or higher than 126fF.

The corresponding electrical model is slightly modified with the addition of a MIM capacitor, as shown in

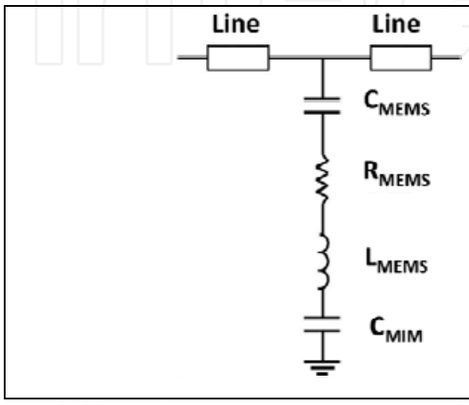

Components	Values
Line (µm)	105
LMEMS (pH)	23,5
CVAR(fF) up down	110 500
RMEMS (Ω) up down	2 0,15
Q@ 20GHz up down	36 106
CMIM(fF)	450

Table 2. Electrical model of varactor with MIM capacitors

The MIM capacitor's value corresponds to 450fF, which leads to varactor's values (MEM and MIM capacitors in serial configuration) of 110 and 500fF in the up and down states respectively. It results in a capacitive ratio of 4.5 (Bordas, 2008).
Vähä-Heikkilä et al. have proposed another solution for the reduction and control of the capacitor ratio. They used Metal-Air-Metal (MAM) capacitors with RF-MEMS attractors (see figure 12), which results in higher quality factor, as no dielectric losses appear in the MAM device. This results in a 150% improvement in the off-state quality factor, a value of 154 was indeed obtained at 20GHz (Vähä-Heikkilä & Rebeiz 2004-a) with MAM capacitors 100 times larger than MIM ones.

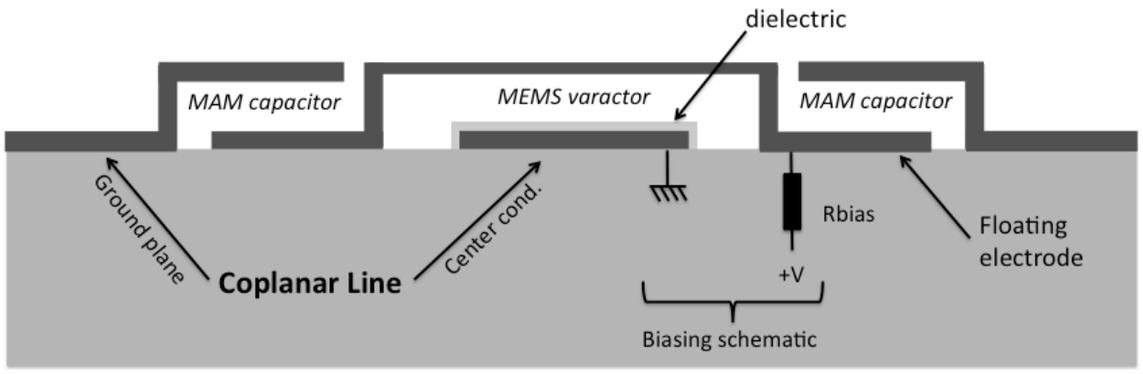

Fig. 12. Metal-Air-Metal (MAM) capacitor associated with RF-MEMS varactors used for tuning elements in tuner (Vähä-Heikkilä & Rebeiz 2004-a)

Despites these possible quality factors' improvements, quality factors higher or around 30-40 are sufficient to achieve low losses' tuners, as suggested by the figure 7. RF-MEMS devices are consequently well adapted to tuner applications (and more generally all reconfigurable applications) as they also exhibit:

(1) Controllable and predictable capacitor ratios in the range of 2-5:1,
(2) Medium power capabilities,
(3) Compatibility with a system-on-chip approach,
(4) Low intermodulation.

The next paragraph then presents an explicit method to design an RF-MEMS-based tuner.

4. RF-MEMS Tuner Design methodology: example of the design of a building block

4.1 Efficient Design Methodology

Thanks to the RF-MEMS-varactors and associated technology presented in the last paragraph, we propose to detail and illustrate an explicit design methodology of TL-based impedance tuner. The design and characterization of a basic building block of tuner: a single stub architecture, presented in the figure 13, is detailed and discussed. The investigated structure is composed of 3 TL sections: 2 input/output accesses and 1 stub. Each line is loaded by 2 switchable varactors. When the loading capacitance is increased, the line electrical length is increased and the matching is tuned. Reconfigurable varactors can be realizable thanks to a switch, which address 2 different capacitors, or by the association of fixed and tunable capacitors as illustrated in the figure 13.

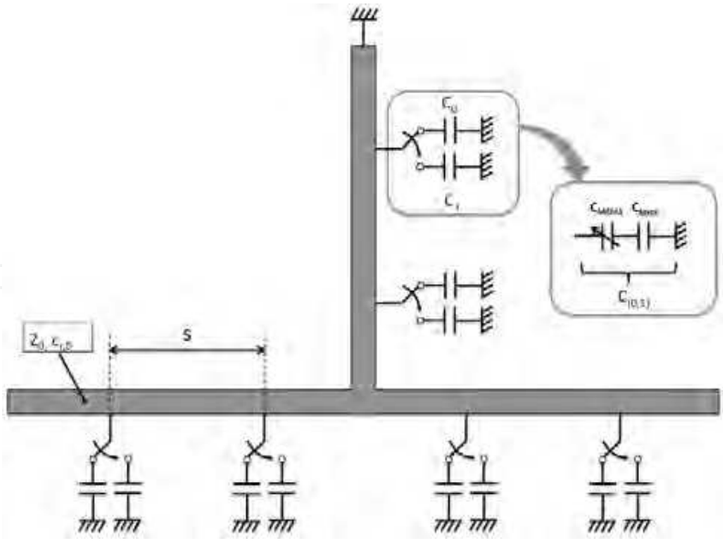

Fig. 13. Tuner's Topology

The parameters, which have to be optimized, are:

- the MIM capacitor value : C_{MIM} (we consider that the MEMS capacitor – without the MIM- is fixed by the technological constraints),
- the characteristic impedance of the unloaded line (without the varactors) : Z_0,
- the spacing s between the MEMS capacitor both for the input and the output lines and for the stub.

It follows such targets :

- an impedance coverage:
  1. as uniform as possible : target 1,
  2. providing high values of $|\Gamma|$: target 2,
  3. providing also low values of $|\Gamma|$: target 3,
- Technological feasibility (this limits some dimensions).

The target 3 is fulfilled when the characteristic impedance of the loaded line, with all MEMS in the up position (named $Z_{c,up}$) is close to 50Ω :

$$Z_{c,up} = 50\Omega \tag{1}$$

The first target is difficult to be analytically expressed. To circumvent this difficulty, we propose to consider that this target is reached if, for each tuner's transmission line (TL), presented in the figure 14, the phase difference of the reflection scattering parameter (S_{11}) between the two MEMS states is 90°. Indeed, when a phase difference of 90° is reached for a TL, an half wise rotation is observed in the Smith Chart then leading to "a best impedance coverage".

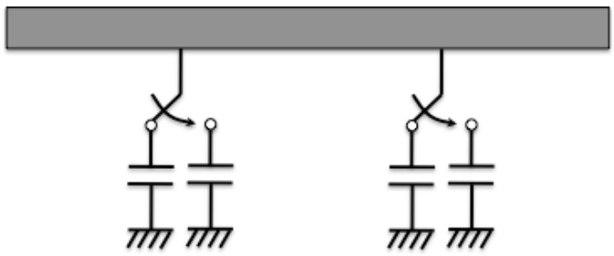

Fig. 14. TL with tunable electrical length. This element corresponds to a generic building block of complex tuner architectures.

To express this constraint, a parameter is introduced, which represents the two-states-difference of the normalized length of TL, regarding the wavelength:

$$\boldsymbol{\delta} = \frac{l}{\lambda_{down}} - \frac{l}{\lambda_{up}} \tag{2}$$

The impedance coverage will then be optimally uniform if:

$$\delta = 1/4 \tag{3}$$

After some mathematical manipulations, the proposed figure of merit can be expressed as a function of the designed parameters:

$$\boldsymbol{\delta} = \frac{f\sqrt{\varepsilon_{r0}}}{c} 2s\left(\sqrt{1 - R + RK_{up}}\right) - \sqrt{K_{up}} \tag{4}$$

where $K_{up}=(Z_0/Z_{c,up})^2$; R, s and ε_{r0} correspond to the capacitor ratio C_{down}/C_{up}, the spacing between varactors and the relative permittivity of the unloaded line respectively.

The design equation (4) then translates into an explicit expression of the capacitor ratio (then named R_{opt}), which permits to design the value of the MIM capacitors of the varactors:

$$\boldsymbol{R_{opt}} = \frac{\left(\frac{\delta}{B} + \sqrt{K_{up}}\right)^2 - 1}{K_{up} - 1} \tag{5}$$

$$B = \frac{f\sqrt{\varepsilon_{reff}}}{c} 2s \tag{6}$$

The optimal value of the MIM capacitor is finally deduced from this optimal capacitor ratio of the varactor and the up-state value of the MEMS devices (without MIM capacitor):

$$C_{MIM}^{opt} \approx (\boldsymbol{R_{opt}} - 1) \times C_{MEMS}^{up} \tag{7}$$

This last expression assumes that the MEMS capacitor ratio is large enough compared with the one of the resulting varactor.

Finally, the target 2 is fulfilled when the down-state capacitor value of the varactor is sufficiently large to 'short circuit the signal', leading to the edge of the Smith Chart. As this value is already defined by the designed equation (4), the target 2 is optimized by tuning the s value, which is -on the other side- constrained by the Bragg condition (Barker & Rebeiz, 1998) and the technological feasibility. The s value will then be a parameter to optimize iteratively in order to reach the best compromise between "wide impedance coverage (i.e. equation (1) and (4)) and "technological feasibility".
This procedure was applied to a single-stub tuner. Considering the RF-MEMS technology presented in the previous paragraph, the values summarized in the table 3 are reached after some iterations and totally defines the tuner of the figure 13.

Transmission line Characteristic Impedance		63Ω
MEMS capacitor (theoretical)	**up**	70 fF
	down	4000 fF
MIM capacitor		500 fF
Total Capacitor	**up**	60 fF
	down	450 fF
Total Capacitor Ratio		7-8

Table 3. Values of the tuner's parameters using the proposed methodology

4.2 Measured RF-Performances

The microphotography in figure 15 presents the fabricated single-stub tuner, whose electrical parameters are given in the table 3. The integration technology used has been developed at the LAAS-CNRS (Grenier et al. 2004; Grenier at al. 2005; Bordas, 2008) and, in order to integrate tuners with active circuits, the RF-MEMS devices were realized on silicon (2kΩ.cm) with a BCB interlayer of 15 µm.

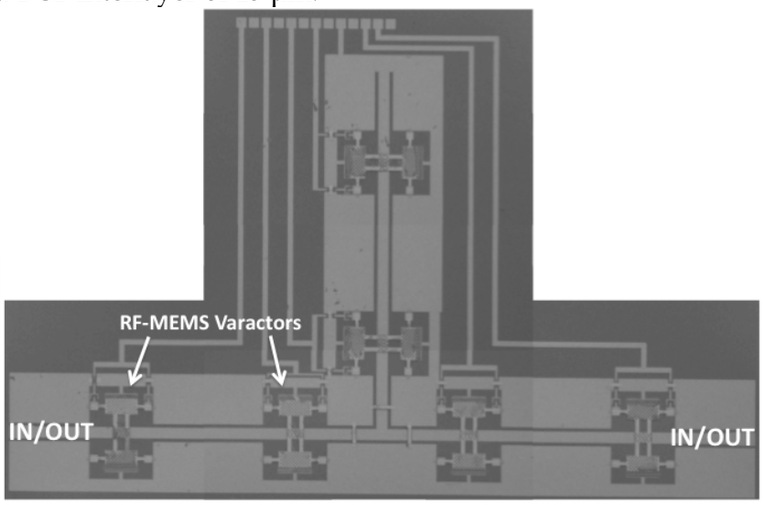

Fig. 15. Micro-photography of the fabricated RF-MEMS single stub tuner (Bordas, 2008)

The on-wafer 2-ports S parameters have been measured from 400 MHz to 30 GHz for the 2^6=64 possible states. The DC feed lines for the varactors actuation have been regrouped and connected to an automated DC –voltages supplier through a probe card (see figure 16).

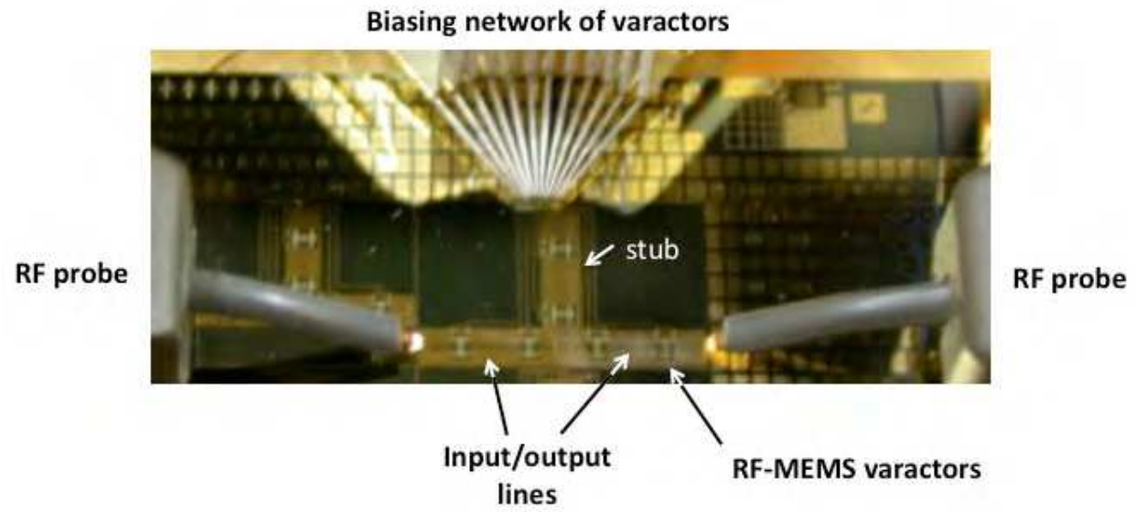

Fig. 16. Micro-photography of the fabricated tuner under testing

The measured and simulated (with Agilent ADS) S_{11} parameters vs frequency, when all the MEMS devices are in the down position, are shown in fig. 17. This demonstrates the accuracy of the RF-MEMS technologies' models over a wide frequency range.
The fig. 18 presents the measured and simulated impedance coverage at 10, 12.4 and 14GHz (64 simulated impedance values and 47 measured ones) with 50 Ω input and output terminations. There is a good agreement between the simulated and measured impedance coverage with high values of $|\Gamma_{MAX}|$ and VSWR parameters as 0.82 and 10 are respectively obtained at 14 GHz.

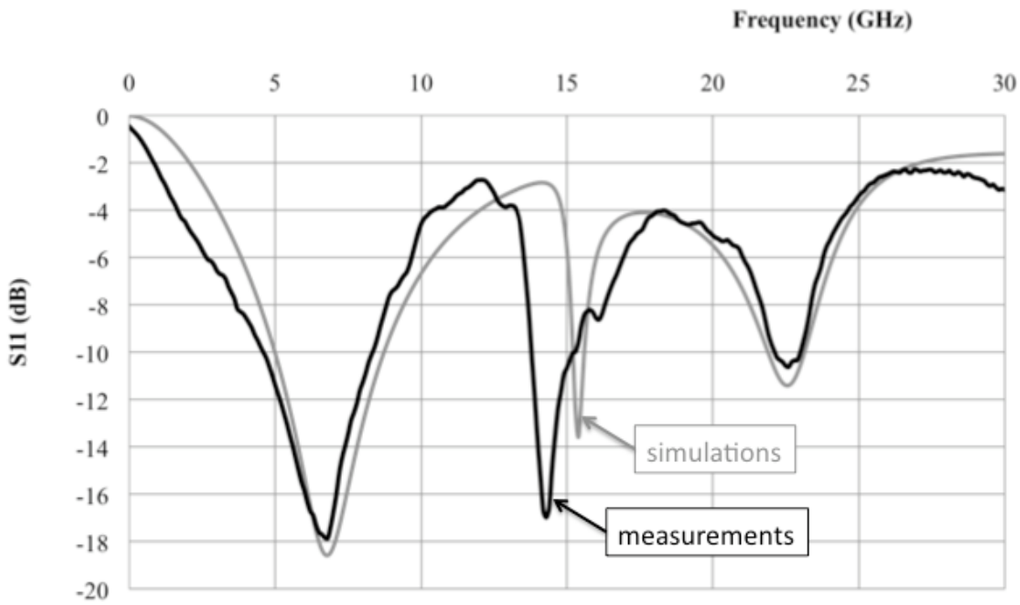

Fig. 17. Measured and simulated S11 parameter, when all MEMS devices are in the down position

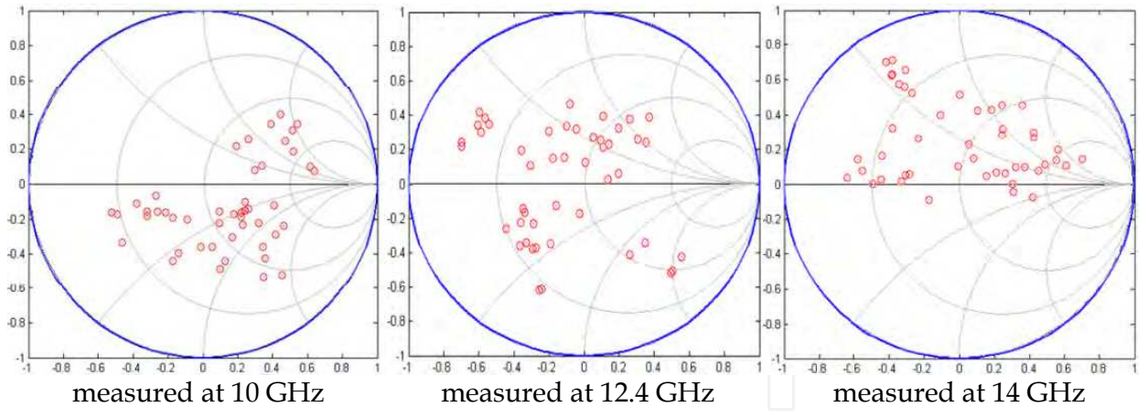

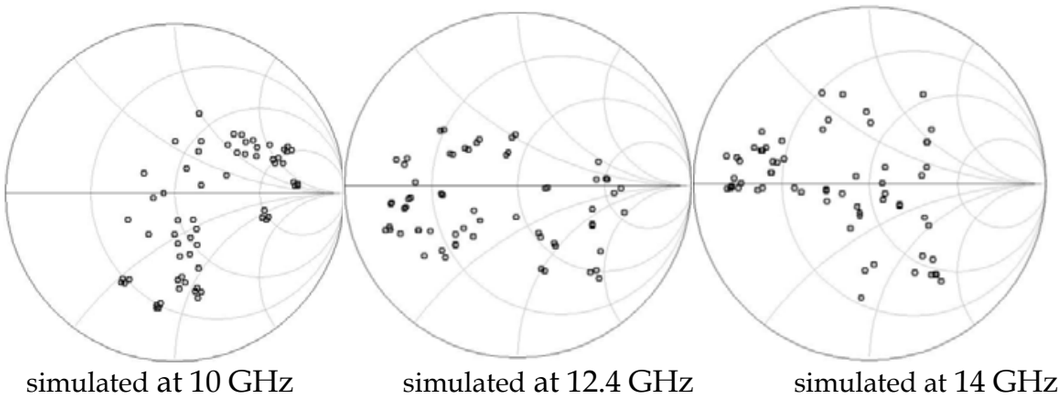

Fig. 18. Measured and simulated impedances coverage of the tuner at 10, 12.4 and 14 GHz

This result then validates the proposed design methodology as a wide impedance coverage is reached after the first set of fabrication.

In term of tunable matching capability of the resulting circuit, the figure 19 presents the input impedances of the fabricated tuner, when the output is loaded by 20 Ω. The results demonstrate that the tuner is able to match 20 Ω on a 100 Ω input impedance (the 100 Ω circle is drawn in the Smith Chart of the figure 19). The corresponding impedance matching ratio of 5:1 is in the range of interest of a wide range of applications, where low noise or power amplifiers and antennas have to be matched under different frequency ranges.

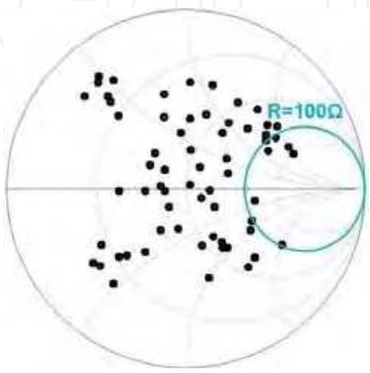

Fig. 19. Predicted input impedance coverage at 20 GHz. The output of the tuner is loaded by 20 Ω.

5. Capabilities of RF-MEMS based tuner

The previous paragraph has presented an illustration of the design of an RF-MEMS-based tuner in Ku and K-bands. Although the considered structure was quite simple (1-stub topology), the measured performances in term of VSWR and impedance coverage was very satisfactory. Of course, the presented design methodology is very generic and can also be applied for the design of more complicated tuner architecture. The figure 20 presents a double and triple stub tunable matching network.

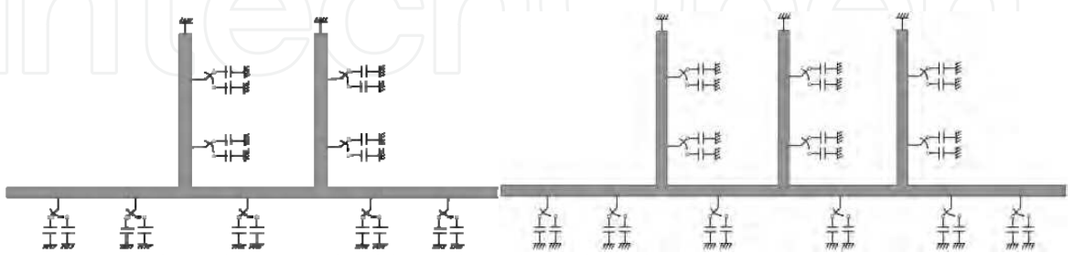

Fig. 20. RF-MEMS based tuner : double and triple stub architecture

Despites the drawbacks of such structures in terms of occupied surface and insertion losses, their impedance coverage and maximum VSWR feature improved values compare to single stub structures. The figure 21 illustrates typical results expected from double and triple stubs tuners and demonstrates the power of the design methodology presented in the paragraph 4 as well as the capabilities of RF-MEMS technologies for the implementation of integrated tuners with high performances. Excellent impedance coverage was indeed predicted as well as high value of reflection coefficient in all the four quadrant of the Smith-Chart.

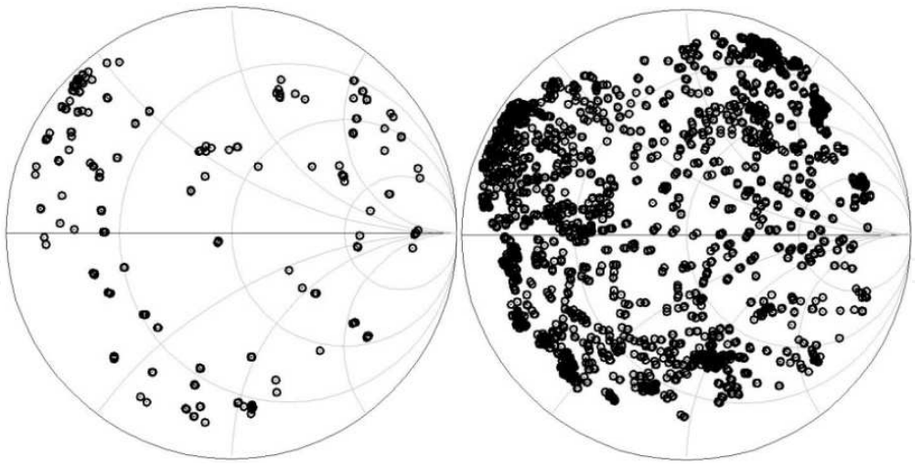

Fig. 21. Predicted impedance coverage of a 9 bits (2 stubs) and 12 bits (3 stubs) RF-MEMS tuner

The simulations predict for both architectures a $|\Gamma_{MAX}|$ value of 0.95 at 20GHz, which corresponds to a VSWR around 40. Compared with MMIC-tuner, RF-MEMS architectures clearly exhibit improvement in term of achievable VSWR. In Ka-band, the losses of FET or Diode limit the VSWR of tuner to 20 (McIntosh et al., 1999; Bischof, 1994), whereas as for RF-

MEMS-technology-based tuners exhibit values ranging from 32 (Kim et al., 2001) to even 199 (Vähä-Heikkilä et al., 2007). It clearly points out the breakthrough obtained by using RF-MEMS technologies for microwave and millimeterwave tuner applications.
Moreover, the demonstration of high RF-performances of RF-MEMS-based tuner have been successfully carried out:
1. on various architectures for

- 1-stub (Vähä-Heikkilä et al., 2004-c; Dubuc et al., 2008; Bordas, 2008; Vähä-Heikkilä et al. 2007),
- 2-stubs (Papapolymerou et al., 2003; Kim et al., 2001; Vähä-Heikkilä et al., 2005; Vähä-Heikkilä et al., 2007)
- 3-stubs (Vähä-Heikkilä et al., 2004-b; Vähä-Heikkilä et al., 2005; Vähä-Heikkilä et al., 2007)
- Distributed TL (Lu et al., 2005; Qiao et al., 2005; Shen & Barker, 2005; Lakshminarayanan & Weller, 2005; Vähä-Heikkilä & Rebeiz, 2004-a)

As anticipated (Collin, 2001), the VSWR rises when the number of stubs increases. The table 4 presents the $|\Gamma_{MAX}|$ and VSWR values for 1, 2 and 3-stubs RF-MEMS tuners. Value around 40 is achieved at 16 GHz for a 3-stub structure, which corresponds to a 100% improvement compare with a 1-stub network, but at the expense of 70% rise of the occupied surface.

Architecture	**1- stub tuner**	**2- stub tuner**	**3-stub tuner**
$\|\Gamma_{MAX}\|$ **@ 16 GHz**	0,91	0,93	0,95
VSWR @ 16 GHz	21	28	39

Table 4. $|\Gamma_{MAX}|$ and VSWR vs tuner architecture (Vähä-Heikkilä et al., 2007)

2. Over a wide frequency range from 4 to 115 GHz :

- C-band (Vähä-Heikkilä & Rebeiz, 2004-a),
- X-band (Vähä-Heikkilä & Rebeiz, 2004-a; Vähä-Heikkilä et al., 2004-b; Qiao et al., 2005),
- Ku-band(Papapolymerou et al., 2003; Vähä-Heikkilä et al., 2006),
- K-band (Dubuc et al., 2008; Bordas, 2008; Shen & Barker, 2005),
- Ka-band (Kim et al., 2001; Lu et al., 2005, Vähä-Heikkilä & Rebeiz, 2004-d),
- U and V-band (Vähä-Heikkilä et al., 2004-c)
- W-band (Vähä-Heikkilä et al., 2005)

One can notice that high values of $|\Gamma_{MAX}|$ and VSWR are generally achieved for high frequency operation. This is suggested by the datas reported in the table 5, which reports a tuner with an optimized impedance coverage at 16 GHz. At this frequency, a VSWR of 28 is measured, whereas at 30 GHz an impressive value of 199 is reported.

Frequency	6 GHz	8 GHz	12 GHz	16 GHz*	20 GHz	30 GHz
$\lvert\Gamma_{MAX}\rvert$	0,95	0,94	0,91	0,93	0,96	0,99
VSWR	39	32	21	28	49	199

* Optimal impedance coverage of the Smith-Chart

Table 5. $\lvert\Gamma_{MAX}\rvert$ and VSWR vs frequency for a 2-stubs tuner (Vähä-Heikkilä et al., 2007)

A tradeoff between impedance coverage and high value of $\lvert\Gamma_{MAX}\rvert$ and VSWR then exists and both features need to be considered for fair comparison.

6. Conclusions

This chapter has presented the design, technology and performances of RF-MEMS-based tuners. Various architectures have been presented in order to give a large overview of tuner-topologies. An efficient and explicit design methodology has been explained and illustrated through a practical example. The authors have moreover outlined the potential of RF-MEMS technologies for different applications (tunable impedance matching between integrated functions within smart microsystems, wide impedance values generations for devices characterization) because of their ability for IC-co-integration, low losses performances and low distortion characteristics.

7. Acknowledgements

The authors would like to specifically acknowledge Chloe Bordas, who was Ph.D student under the supervision of Katia Grenier and David Dubuc from 2005 to 2008 and worked on RF-MEMS based tuner. She was an essential backbone of the work presented in this Chapter.

We also would like to thanks Samuel Melle, Benoît Ducarouge and Jean-Pierre Busquere, Ph. D students under the supervision of David Dubuc and Katia Grenier from 2002 to 2005. Their work on RF-MEMS design, fabrication and reliability contributed to rise the knowledge of the team, and permit to envision circuits based on RF-MEMS varactors.

Katia Grenier and David Dubuc also acknowledge the support of Thales Alenia Space, the French Defense Agency (DGA) and ST-Microelectronics.

8. References

Barker, S. Rebeiz, G.M. (1998). Distributed MEMS true-time delay phase shifters and wide-band switches. *IEEE Transactions on Microwave Theory and Techniques*, Vol. 46, Issue 11, Part 2, Nov. 1998 pp:1881 – 1890

Bischof, W. (1994). Variable impedance tuner for MMIC's. *Microwave and Guided Wave Letters,* Volume 4, Issue 6, June 1994 Page(s):172 – 174

Bordas, C.; Grenier, K.; Dubuc, D.; Paillard, M.; Cazaux, J.-L.; et al. (2007-a). Temperature stress impact on power RF MEMS switches, *Microtechnologies for the new millennium 2007*, Smart sensors, actuators and MEMS, Maspalomas, Espagne. Mai 2007.

Bordas, C.; Grenier, K.; Dubuc, D.; Flahaut, E.; Pacchini, S. Paillard, M.; Cazaux, J-L. (2007-b). Carbon nanotube based dielectric for enhanced RF MEMS reliability. *IEEE/MTT-S International Microwave Symposium*, June 2007.

Bordas, C. (2008). Technological optimization of RF MEMS switches with enhanced power handling – Elaboration of a MEMS-based impedance tuner in K-band. *Ph.D. dissertation* (in French), April 2008.

Busquere, J.-P.; Grenier, K.; Dubuc, D.; Fourn, E.; Ancey, P.; et al. (2006). MEMS IC concept for Reconfigurable Low Noise Amplifier. *36th European,Microwave Conference*, 2006. 10-15 Sept. 2006 Page(s):1358 - 1361

Collin, R. E. (2001). *Field Theory of Guided Waves*, 2nd ed., IEEE Press.

Dubuc, D.; Saddaoui, M; Melle, S.; Flourens, F.; Rabbia, L.; Ducarouge, B.; Grenier, K.; et al. (2004). Smart MEMS concept for high secure RF and millimeterwave communications. *Microelectronics Reliability*, Volume 44, Issue 6, June 2004, Pages 899-907

Dubuc, D.; Bordas , C.; Grenier, K. (2008). Efficient design methodology of RF-MEMS based tuner. *European Microwave Week 2008 (EuMW 2008)*, Amsterdam (Pays Bas), 27-31 Octobre 2008, pp.398-401

Ducarouge, B.; Dubuc, D.; Melle, S.; Bary, L.; Pons, P.; et al. (2004). Efficient design methodology of polymer based RF MEMS switches. *2004 Topical Meeting on Silicon Monolithic Integrated Circuits in RF Systems, 2004*. 8-10 Sept. 2004 Page(s):298 – 301

Goldsmith, C.L.; Forehand, D.I.; Peng, Z.; Hwang, J.C.M.; Ebel, I.L. (2007). High-Cycle Life Testing of RF MEMS Switches. *IEEE/MTT-S International Microwave Symposium, 2007*. 3-8 June 2007 Page(s):1805 – 1808.

Grenier, K.; Dubuc, D.; Mazenq, L.; Busquère, J-P.; Ducarouge, B.; Bouchriha, F.; Rennane, M.; Lubecke, V.; et al. (2004). Polymer based technologies for microwave and millimeterwave applications. *50th IEEE International Electron Devices Meeting, 2004*, San Francisco, USA, Dec. 2004.

Grenier, K.; Dubuc, D.; Ducarouge, B.; Conedera, V.; Bourrier, D.; Ongareau, E.; Derderian, P.; et al. (2005). High power handling RF MEMS design and technology. *18th IEEE International Conference on Micro Electro Mechanical Systems,* 2005. 30 Jan.-3 Feb. 2005 Page(s):155 – 158

Grenier, K.; Bordas, C. Pinaud, S.; Salvagnac, L.; Dubuc, D. (2007). Germanium resistors for RF MEMS based Microsystems. *Microsystems Technologies,* DOI 10.1007/s00542-007-0448-4.

Kim, H.-T.; Jung, S.; Kang, K.; Park, J.-H.; Kim, Y.-K.; Kwon Y. (2001). Low-loss analog and digital micromachined impedance tuners at the Ka-band. *IEEE Transactions on Microwave Theory and Techniques*, December 2001, Vol. 49, No. 12, pp. 2394-2400.

Lakshminarayanan, B.; Weller, T. (2005). Reconfigurable MEMS transmission lines with independent Z0- and β- tuning. *IEEE/MTT-S International Microwave Symposium*, 2005.

Lu, Y.; Katehi, L. P. B.; Peroulis D. (2005). High-power MEMS varactors and impedance tuners for millimeter-wave applications. *IEEE Transactions on Microwave Theory and Techniques*, November 2005, Vol. 53, No. 11, pp. 3672-3678.

McIntosh, C.E.; Pollard, R.D.; Miles, R.E. (1999). Novel MMIC source-impedance tuners for on-wafer microwave noise-parameter measurements. *IEEE Transactions on Microwave Theory and Techniques*, Volume 47, Issue 2, Feb. 1999 Page(s):125 – 131

Melle, S.; De Conto, D.; Dubuc, D.; Grenier, K.; Vendier, O.; Muraro, J.-L.; Cazaux, J.-L.; et al. (2005). Reliability modeling of capacitive RF MEMS. *IEEE Transactions on Microwave Theory and Techniques*, Volume 53, Issue 11, Nov. 2005 Page(s):3482 - 3488

Papapolymerou, J.; Lange, K.L.; Goldsmith, C.L.; Malczewski, A.; Kleber, J. (2003). Reconfigurable double-stub tuners using MEMS switches for intelligent RF front-end. *IEEE Transactions on Microwave Theory and Techniques*, Volume 51, Issue 1, Part 2, Jan. 2003 Page(s):271 - 278

Pozar, D.M. (2005). *Microwave Engineering*. 3rd ed., Wiley 2005.

Qiao, D.; Molfino, R.; Lardizabal, S.M.; Pillans, B.; Asbeck, P.M.; Jerinic, G. (2005). An intelligently controlled RF power amplifier with a reconfigurable MEMS-varactor tuner. *IEEE Transactions on Microwave Theory and Techniques*, Volume 53, Issue 3, Part 2, March 2005 Page(s):1089 - 1095

Rebeiz, G. M. (2003). *RF MEMS: Theory, Design, and Technology*. New York: Wiley, 2003.

Shen, Q; Baker, N.S. (2005). A reconfigurable RF MEMS based double slug impedance tuner. *European Microwave Conference 2005*, Paris, pp. 537-540.

Tagro, Y.; Gloria, D.; Boret, S.; Morandini, Y.; Dambrine, G. (2008). In-situ silicon integrated tuner for automated on-wafer MMW noise parameters extraction of Si HBT and MOSFET in the range 60–110GHz. *72nd ARFTG Microwave Measurement Symposium*, 2008. 9-12 Dec. 2008 Page(s):119 – 122

Van Spengen, W.M.; Puers, R.; Mertens, R.; De Wolf, I. (2002). Experimental characterization of stiction due to charging in RF MEMS. *International Electron Devices Meeting, 2002.* IEDM '02. Digest. 8-11 Dec. 2002 Page(s):901 – 904

Vähä-Heikkilä, T.; Rebeiz, G.M. (2004-a). A 4-18-GHz reconfigurable RF MEMS matching network for power amplifier applications. *International Journal of RF and Microwave Computer-Aided Engineering*. Volume 14 Issue 4, Pages 356 – 372. 9 Jun 2004

Vähä-Heikkilä, T.; Varis, J.; Tuovinen, J.; Rebeiz, G. M. (2004-b). A reconfigurable 6-20 GHz RF MEMS impedance tuner". *IEEE/MTT-S International Microwave Symposium*, 2004, pp. 729-732.

Vähä-Heikkilä, T.; Varis, J.; Tuovinen, J.; Rebeiz, G.M. (2004-c). A V-band single-stub RF MEMS impedance tuner. *34th European Microwave Conference, 2004*, Volume 3, 11-15 Oct. 2004 Page(s):1301 – 1304

Vähä-Heikkilä, T.; Rebeiz, G. M. (2004-d). A 20-50 GHz reconfigurable matching network for power amplifier applications. *IEEE/MTT-S International Microwave Symposium*, 2004, pp. 717-720.

Vähä-Heikkilä, T.; Varis, J.; Tuovinen, J.; Rebeiz, G.M. (2005).W-band RF MEMS double and triple-stub impedance tuners. *IEEE/MTT-S International Microwave Symposium*, 12-17 June 2005

Vähä-Heikkilä, T.; Caekenberghe, K.V.; Varis,J.; Tuovinen, J.; Rebeiz, G.M. (2007). RF MEMS Impedance Tuners for 6-24 GHz Applications. *International Journal of RF and Microwave Computer-Aided Engineering*, 26 Mar 2007, Volume 17 Issue 3, Pages 265 – 278.

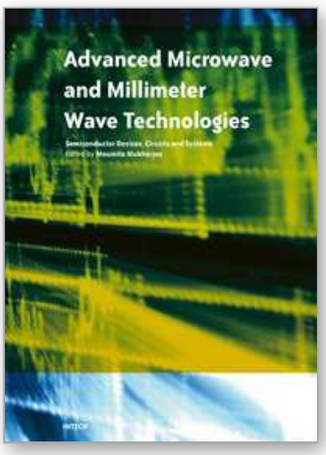

Advanced Microwave and Millimeter Wave Technologies
Semiconductor Devices Circuits and Systems
Edited by Moumita Mukherjee

ISBN 978-953-307-031-5
Hard cover, 642 pages
Publisher InTech
Published online 01, March, 2010
Published in print edition March, 2010

This book is planned to publish with an objective to provide a state-of-the-art reference book in the areas of advanced microwave, MM-Wave and THz devices, antennas and systemtechnologies for microwave communication engineers, Scientists and post-graduate students of electrical and electronics engineering, applied physicists. This reference book is a collection of 30 Chapters characterized in 3 parts: Advanced Microwave and MM-wave devices, integrated microwave and MM-wave circuits and Antennas and advanced microwave computer techniques, focusing on simulation, theories and applications. This book provides a comprehensive overview of the components and devices used in microwave and MM-Wave circuits, including microwave transmission lines, resonators, filters, ferrite devices, solid state devices, transistor oscillators and amplifiers, directional couplers, microstripeline components, microwave detectors, mixers, converters and harmonic generators, and microwave solid-state switches, phase shifters and attenuators. Several applications area also discusses here, like consumer, industrial, biomedical, and chemical applications of microwave technology. It also covers microwave instrumentation and measurement, thermodynamics, and applications in navigation and radio communication.

InTech Europe
University Campus STeP Ri
Slavka Krautzeka 83/A
51000 Rijeka, Croatia
Phone: +385 (51) 770 447
Fax: +385 (51) 686 166
www.intechopen.com

InTech China
Unit 405, Office Block, Hotel Equatorial Shanghai
No.65, Yan An Road (West), Shanghai, 200040, China
中国上海市延安西路65号上海国际贵都大饭店办公楼405单元
Phone: +86-21-62489820
Fax: +86-21-62489821

IntechOpen